



SMR.703 - 7

**WORKING PARTY ON
MECHANICAL PROPERTIES OF INTERFACES**

23 AUGUST - 3 SEPTEMBER 1993

"Semiconductor Multilayers"

**"Misfit Dislocations in Strained Layer Epitaxy:
I. Energetics"
(Part III)**

**R. HULL
AT&T Bell Laboratories
600 Mountain Avenue
Murray Hill, NJ 07974-0636
U.S.A.**

These are preliminary lecture notes, intended only for distribution to participants.

MISFIT DISLOCATIONS IN STRAINED LAYER EPITAXY: I. ENERGETICS

R. Hull and J.C. Bean
AT&T Bell Laboratories,
600 Mountain Avenue, Murray Hill, NJ 07974

(Received June 23, 1992)
(Revised July 15, 1992)

Introduction

In this paper and a companion paper in this volume ("Misfit Dislocations in Strained Layer Epitaxy: II Kinetics"), we summarize the energetic and kinetic factors which govern stress relaxation by misfit dislocations in strained layer epitaxy. We base theoretical descriptions of these processes upon (i) classic models of dislocation structure and motion (e.g. Ref. 1), (ii) the Mechanical Equilibrium model of Matthews and Blakeslee (2) for predicting the epitaxial layer dimensions at which misfit dislocations are energetically favored and (iii) the kinetic model of Dodson and Tsao (3) for predicting strain relaxation rates. Experimental data is drawn from the literature and from our own observations of dislocation microstructures and kinetics obtained from in-situ strained layer relaxation experiments in a transmission electron microscope (TEM) (4,5).

Geometrical and Energetic Considerations

We shall consider in these papers planar strained layer structures, where the epitaxial layer is grown upon a planar substrate of orientation (hkl) and is bounded either by a free surface or by a planar capping layer of the same material as the substrate. (The more general case of strain relaxation in non-planar epitaxial growth has been considered by several authors, e.g. Refs. 6,7,8,9,10. Non-planar geometries are also clearly very pertinent to electronic device structures).

Considering an uncapped structure, Figure 1(a), interfacial misfit dislocation length is generally created by glide of dislocations on the most widely spaced atomic planes, where the Peierls stress is lowest (1). The propagating dislocation will consist of a growing interfacial misfit segment bounded by moving "threading" segments traversing the epitaxial layer. (These threading segments may be annihilated at the edge of the substrate wafer or by interaction with other defects). In general, it is expected that the Burgers vector of these dislocations will be such that they lie within the primary slip system of the epitaxial layer, although dislocations with Burgers vectors lying out of the glide plane are often observed in systems with high lattice mismatch or high dislocation densities (e.g. 11,12) - these are generally ascribed to reactions of constituent glide dislocations, or to introduction at growing island edges. In Figure 1(b), we show the geometry pertinent to capped strained layers. In this case, the dislocation generally propagates with interfacial segments at both interfaces, with threading arms traversing the epitaxial layers. Note that if the capping layer is sufficiently thin, however, propagation analogous to the uncapped case may be observed, with the misfit segment at the lower epitaxial interface only. The conditions for single or double interfacial segments in buried strained layers have been analyzed by Twigg (13); it is found that for most cases where the capping layer thickness is greater than the epilayer thickness, then the double interfacial segment is observed.

In both capped and uncapped structures, dislocations propagate because they relax the stress due to lattice mismatch in the epitaxial layer. The energetic balance between the strain energy relieved and the self energy of the misfit dislocation array was addressed several decades ago by Frank and van der Merwe (14). This led to the concept of a critical epitaxial layer thickness, h_c , below which the self energy of the dislocation array exceeds that of the strain energy relaxed, and thus an undislocated epilayer is expected. A somewhat simpler description of the critical thickness was developed by Matthews and Blakeslee (MB) (2), who considered the balance between the force due to the lattice mismatch acting on the propagating threading arm with a "line tension" term due to the self energy of the extra interfacial dislocation length created. We shall describe the MB theory in terms of stresses rather than forces for consistency with the concept of excess stress developed by Dodson and Tsao (DT) (3).

The resolved shear stress acting on the dislocation threading arm is given by:

$$\sigma_a = 2GSe \frac{(1+\nu)}{(1-\nu)} \quad (1)$$

Here G is the epilayer shear modulus, ν the epilayer Poisson ratio, and ϵ is the lattice mismatch strain between epilayer and substrate. The quantity S is known as the Schmid factor (15) and resolves the lattice mismatch stress onto the dislocation Burgers vector according to the equation:

$$S = \cos\lambda\cos\phi \quad (2)$$

where λ is the angle between the dislocation Burgers vector and the line in the interface which is normal to the dislocation line direction and ϕ is the angle between the slip plane and the normal to the interface. Note that these angular factors ensure that only dislocations lying within slip planes *inclined* to the interface (i.e. not parallel or perpendicular to it) will experience the lattice mismatch stress.

The "line tension stress" is derived from the self energy of a dislocation a distance h from a free surface (1), yielding:

$$\sigma_T = \frac{Gb\cos\phi(1-\nu\cos^2\theta)}{4\pi h(1-\nu)} \ln(\alpha \frac{h}{b}) \quad (3)$$

Here b is the magnitude of the dislocation Burgers vector, θ is the angle between b and the dislocation line direction, h is the epilayer thickness and α is a term attempting to describe the core energy of the dislocation (which for many materials, particularly covalently bonded semiconductors, is not accurately known).

The MB definition of critical thickness is found by setting $\sigma_a = \sigma_T$ and solving for $h=h_c$. The DT excess stress, $\sigma_{ex} = \sigma_a - \sigma_T$.

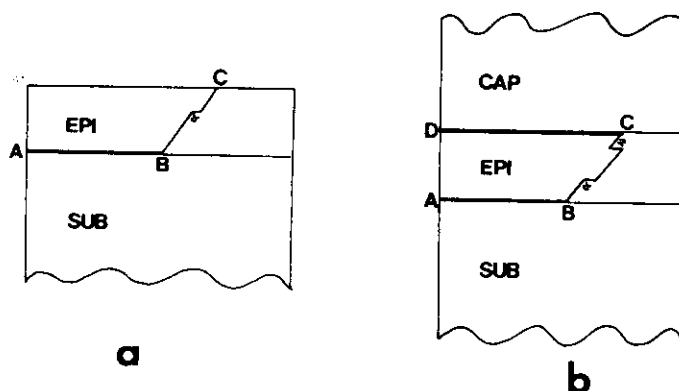


Figure 1: Schematic illustrations of misfit/threading dislocation configurations in (a) uncapped epilayers (b) capped epilayers.

The geometry and microstructure of the misfit dislocation array may now be predicted for a given system and interface orientation (hkl). For simplicity, we will initially assume elastic isotropy and operation of the primary slip system. The line directions of the interfacial dislocations will be given by $u_i = [hkl] \times [p_i q_i r_i]$, where $\{p_i q_i r_i\}$ are the indices of the primary slip planes inclined to the interface. We have tested this prediction for the $Ge_x Si_{1-x}/Si$ (100), (110), (111) and (211) systems. (These materials are diamond cubic and the primary slip planes are {111}. The preferred Burgers vectors, as will be justified later, are $a/2\langle 011 \rangle$ and there are 3 possible orientations of these Burgers vectors in each glide plane - although for some orientations one of these possible Burgers vectors will be a screw dislocation and will not experience a lattice mismatch force from eqn. (2)). As shown in Figure 2, the (100), (110) and (111) interfaces exhibit the expected interfacial dislocation geometries. For these low index planes, misfit dislocations propagating along the directions of all possible intersections of inclined glide planes with a given interface have identical Schmid factors (these Schmid factors, however, vary significantly from interface to interface). In general, for higher index surfaces, {111} planes may intersect along [011], [231] and [213] directions. The Schmid factor is 0.17 for all glide $a/2\langle 011 \rangle$ Burgers vectors intersecting along the [011] direction, but for the $\langle 231 \rangle$ directions, the Schmid factors vary

from 0.13 to 0.26 to 0.40 for the three different possible $a/2\langle 101 \rangle$ glide dislocations for each intersection. The (211) interface would thus be expected to initially relax via dislocation introduction along the two $\langle 231 \rangle$ intersections only, as illustrated for the $\text{Ge}_x\text{Si}_{1-x}/\text{Si}$ system in Figure 3. This interface has also been studied by Mitchell and Unal (16) for the $\text{In}_x\text{Ga}_{1-x}\text{As}/\text{GaAs}$ system.

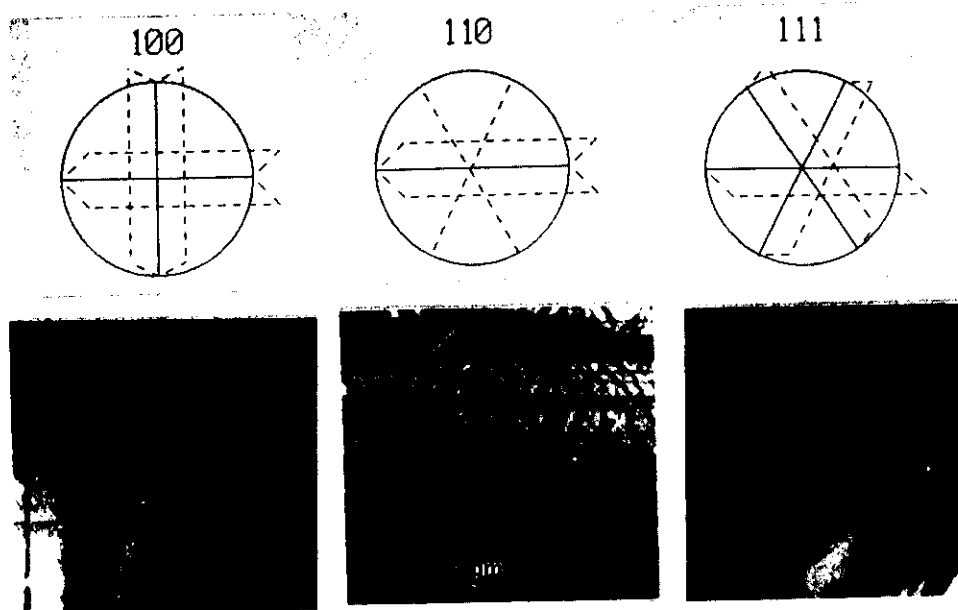


Figure 2: Schematic illustration and experimental verification (by plan view TEM of $\text{Ge}_x\text{Si}_{1-x}/\text{Si}$) of the expected geometries of misfit dislocations at (100), (110) and (111) interfaces. In the schematic illustrations, {111} glide planes are shown intersecting the different surfaces. Intersections of inclined glide planes, corresponding to interfacial misfit dislocation line directions, are shown by straight solid lines.



Figure 3: Misfit dislocations along interfacial $\langle 231 \rangle$ directions at a $\text{Ge}_x\text{Si}_{1-x}/\text{Si}(211)$ interface.

Total vs. Partial Misfit Dislocations

The misfit dislocation Burgers vector is controlled by the crystal structure of the epitaxial layer and by the interface orientation. If the dislocation is to be perfect, the Burgers vector is expected to be the minimum lattice translation vector. For fcc, dc and zb crystals, this corresponds to $\underline{b} = a/2\langle 110 \rangle$, with three different possible variants on each glide plane (as stated above, however, if the interfacial line direction of the misfit segment is $\langle 011 \rangle$, one of these three possible Burgers vectors will be in the screw orientation and will experience no resolved lattice mismatch stress). For fcc, dc and zb crystals, this minimum lattice translation vector is almost invariably observed for perfect dislocations.

In general, however, one should also consider the possibility of partial misfit dislocations, either as separate entities, or as a result of dissociation of perfect dislocations. For 60-degree $a/2\langle 110 \rangle$ dislocations in the fcc, dc and zb systems, the classic dissociation is into Shockley partials (17) following the reaction:

$$\frac{a}{2}\langle 110 \rangle = \frac{a}{6}\langle 121 \rangle + \frac{a}{6}\langle 21\bar{1} \rangle \quad (4)$$

For interfacial line directions $\langle 011 \rangle$, $\cos \lambda$ is 0.50 for the $a/2\langle 110 \rangle$ dislocation and 0.29 and 0.58 for the two $a/6\langle 112 \rangle$ partials (note that the second partial in the above equation is of pure edge type, making its identification by standard $g \cdot b$ analysis (18) in TEM straight-forward). The angles between the Burgers vectors and the interfacial line directions are 60°, 30° and 90° respectively. All of these dislocations may glide within the parent glide plane of the total dislocation. The excess stress acting on these three different dislocations may be calculated from equations (1)-(3), with an extra term $\sigma_{SF} = \gamma/b$ included to take into account the stacking fault energy per unit area, γ , produced by the partial dislocations. In the fcc, dc and zb structures, the Shockley partial dislocation advances or retreats the cubic stacking order by one position, i.e. the stacking sequence ABCAB is transformed to BCABC or CABCA (in equation (4) one of the partials advances the stacking order and one retreats it). The direction of this transformation is crucial: considering the stacking fault within the stacking sequence ABCABCA, the two possible types of stacking fault from passage of a Shockley partial will be ABCA/CAB and ABCA/ABC, where / denotes the stacking fault. The latter configuration will have an extremely high fault energy as it involves nearest-neighbor stacking violations, whereas the former configuration with only second-nearest neighbor stacking violations will be of relatively low energy - of the order $\gamma = 50 - 80 \text{ mJ} \cdot \text{m}^{-2}$ for Si and Ge (19). Calculation of eqns. (1)-(3) shows that the combination of the higher Schmid factor and lower Burgers vector can produce a higher excess stress on the 90-degree partial than the 60-degree total dislocation, even with the extra stress due to the second nearest neighbor stacking fault energy incorporated (the excess stress on the 30-degree partial is generally lowest). This is illustrated in Figure 4 by critical thickness calculations for the $\text{Ge}_x\text{Si}_{1-x}/\text{Si}(110)$ system. Note that the calculated critical thickness for the partial dislocation depends very strongly upon the stacking fault energy assumed (there is also a significantly weaker dependence upon the core energy parameter, α). Even when h_c is greater for the 90° than the 60° dislocation, as the epitaxial layer thickness increases, the stacking fault energy for the partial dislocation becomes more significant, and a thickness, h_x , may be reached at which the excess stress on the 60° total dislocation equals that on the 90° partial dislocation. At increasing thickness beyond h_x , the excess stress on the 60° dislocations becomes progressively greater than on the 90° dislocation.

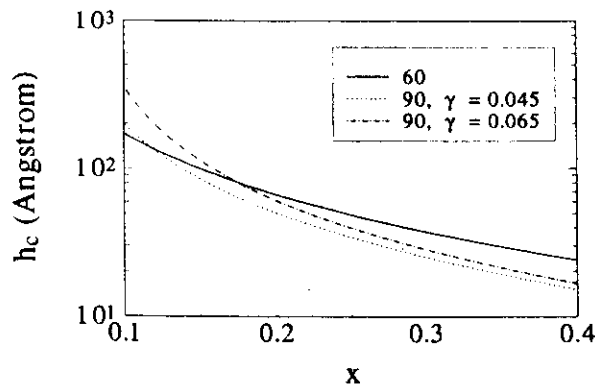


Figure 4: Calculated critical thicknesses (using $\alpha=2$) for 60° total and 90° partial misfit dislocations at the $\text{Ge}_x\text{Si}_{1-x}/\text{Si}(110)$ interface. Calculations for 90° dislocations with different values of stacking fault energy, γ , in $\text{J} \cdot \text{m}^{-2}$ are also shown.

Experimental determination of h_x can yield a very accurate estimate of stacking fault energy, as illustrated in Figure 5 for the $\text{Ge}_x\text{Si}_{1-x}/\text{Si}(110)$ system. It can be seen from this figure that for an assumed value of core energy parameter, $\alpha = 2$, the range of possible stacking fault values consistent with our experimental data is $0.055 < \gamma < 0.075 \text{ Jm}^{-2}$. Note that we show experimental data for both as-grown samples (MBE-growth at 550°C) and for samples which have been post-growth annealed to 750°C for 30 minutes. The significance of the latter set of samples is that virtually all observable post-growth relaxation occurs during this annealing cycle; thus, we are approaching as close to equilibrium as is practical. The much weaker dependence of h_x upon α ensures that this estimate is valid over a range of α from 0.5 - 5 (20), yielding $\gamma = 0.065 \pm 0.010 \text{ Jm}^{-2}$ independent of any reasonable estimate of α and of any reasonable variation of α between the total and partial dislocation cores.

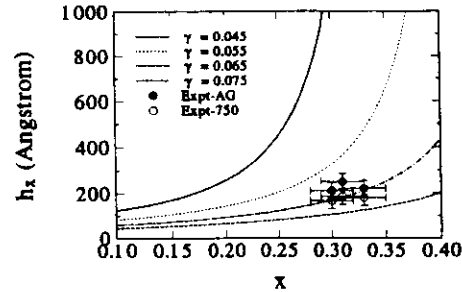


Figure 5: Calculations of the epitaxial layer thickness at which the excess stresses on 60° and 90° dislocations are equivalent, h_x , (assuming $\alpha=2$) for different values of stacking fault energy, γ , on the $\text{Ge}_x\text{Si}_{1-x}/\text{Si}(110)$ surface, together with experimental measurements for as-grown structures, "AG", and samples post-growth annealed at 750°C for 30 minutes, "750".

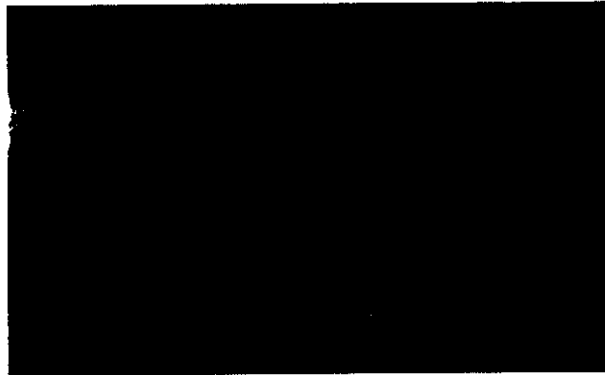


Figure 6: Plan view TEM image of a $(\text{Al})\text{GaAs}/20 \text{ nm } \text{In}_{0.4}\text{Ga}_{0.6}\text{As}/\text{GaAs}(100)$ structure illustrating arrays of interfacial dislocations along interfacial $\langle 011 \rangle$ and $\langle 010 \rangle$ directions.

Operation of other Slip Systems

The assumption that strain relaxation by misfit dislocations will proceed by the minimum Peierl's stress glide system and by that glide dislocation which experiences the maximum excess stress is valid for semiconductor heterostructures (from our own experience and from a survey of the literature) up to applied stresses of the order of a few GPa. There is some evidence, however, that when $\sigma_a > \sim 3 \text{ GPa}$, new slip systems may operate. Thus, as reported in (21),(22), we have observed interfacial dislocation line directions of $u = \langle 010 \rangle$ in $(\text{Al})\text{GaAs}/\text{In}_x\text{Ga}_{1-x}/\text{GaAs}(100)$ heterostructures with $x \geq 0.4$. Such defects are illustrated in Figure 6. We have demonstrated that these are $a/2\langle 101 \rangle$ dislocations gliding on $\{110\}$ planes. This slip system has previously been observed in some metals (23),(24), in bulk GaAs (25) and more recently in the $\text{Ge}_x\text{Si}_{1-x}/\text{Si}(100)$ system with $x > \sim 0.7$ (26). The resolved applied stress required for the secondary $\{110\}$ slip system to become operative is thus about 3 GPa in both the $\text{In}_x\text{Ga}_{1-x}\text{As}/\text{GaAs}$ and $\text{Ge}_x\text{Si}_{1-x}/\text{Si}$ systems. Application of equations (1) and (2) show that the lattice mismatch stress is resolved more efficiently onto the dislocation Burgers vector for the $\{110\}$ vs. $\{111\}$ slip system ($\cos \lambda = 0.71$ for $\{110\}$ vs. 0.50 for $\{111\}$ and $S = 0.58$ vs. 0.41). At these very high stresses, the increase in the applied stress may compensate for the increase in the Peierl's

stress on the more closely packed {110} planes. A quantitative analysis of these arguments will be published in (27).

Conclusions

In this paper we have discussed the geometrical and energetic factors governing strain relaxation by misfit dislocations at strained heteroepitaxial semiconductor interfaces. Kinetic factors will be considered in a companion paper. For the $\text{Ge}_x\text{Si}_{1-x}/\text{Si}$ system, we have shown that simple application of glide plane and interface geometries and the role of the Schmid factor in resolving the lattice mismatch stress generally correctly predicts the interfacial dislocation geometries and Burgers vectors for the (100), (110), (111) and (211) interfaces. For interfaces other than (100), relaxation by $a/6\langle 112 \rangle$ partial dislocations has to be considered as a possible strain relief mechanism. For the (110) surface, consideration of the regimes in which total or partial misfit dislocations are expected to dominate allows the stacking fault energy in $\text{Ge}_x\text{Si}_{1-x}$ alloys with $x=0.3$ to be determined as $\gamma=0.065\pm0.010\text{Jm}^{-2}$. At sufficiently high stresses ($\sim 3\text{ GPa}$), new {110} glide systems are observed for both the $\text{In}_x\text{Ga}_{1-x}\text{As}/\text{GaAs}(100)$ and $\text{Ge}_x\text{Si}_{1-x}/\text{Si}(100)$ systems.

Acknowledgments

We would like to acknowledge experimental collaboration and/or invaluable discussions with: Don Bahnck, Janet Bonar, Connor Buescher, Len Feldman, Eric Kvam (Purdue U.), Roger Malik, Larry Peticolas, Frank Unterwald, John Walker, Ya-Hong Xie, Bonnie Weir

References

- (1) J.P. Hirth and J. Lothe "Theory of Dislocations" (McGraw-Hill, New York, 1968)
- (2) J.W. Matthews and A.E. Blakeslee, *J. Cryst. Growth* 27, 118 (1974); J.W. Matthews, *J. Vac. Sci. Technol.* 12, 126 (1975) and references contained therein.
- (3) B.W. Dodson and J.Y. Tsao, *Appl. Phys. Lett.* 51, 1325 (1987)
- (4) R. Hull, J.C. Bean, D. Bahnck, L.J. Peticolas, K.T. Short and F.C. Unterwald, *J. Appl. Phys.* 70, 2052 (1991)
- (5) R. Hull, J.C. Bean, D.J. Werder and R.E. Leibenguth, *Phys. Rev. B* 40, 1681 (1989)
- (6) M. Grabow and G. Gilmer, *Mat. Res. Soc. Proc.* 94, 13 (1987)
- (7) S. Luryi and E. Suhir, *Appl. Phys. Lett.* 49, 140 (1988)
- (8) R. Hull and A. Fischer-Colbrie, *Appl. Phys. Lett.* 50, 851 (1987)
- (9) D.J. Eaglesham and M. Cerullo, *Phys. Rev. Lett.* 64, 1943 (1990)
- (10) C.W. Synder, B.G. Orr, D. Kessler and L.M. Sander, *Phys. Rev. Lett.* 66, 3032 (1991)
- (11) E.A. Fitzgerald, P.D. Kirchner, G.D. Petit, J.M. Woodall and D.G. Ast, in "Interfacial Defects in Semiconductors", ed. K. Rajan, J. Narayan and D. Ast (The Metallurgical Society, Warrendale, PA, 1988) pp. 173-187
- (12) E.P. Kvam, D.M. Maher and C.J. Humphreys, *J. Mat. Res.* 5, 1900 (1990)
- (13) M.E. Twigg, *J. Appl. Phys.* 68, 5109 (1990)
- (14) F.C. Frank and J.H. van der Merwe, *Proc. Roy. Soc. A* 198, 205; A198, 216; A200, 125 (1949)
- (15) E. Schmid, *Z. Elektrochem* 37, 447 (1931)
- (16) T.E. Mitchell and O. Unal, *J. Elec. Mat.* 20, 723 (1991)
- (17) R.D. Heidenreich and W. Shockley in, "Report on a Conference on Strength of Solids", p. 57 (Physical Society, London, 1948)
- (18) P.B. Hirsch, A. Howie, R.B. Nicholson, D.W. Pashley and M.J. Whelan, "Electron Microscopy of Thin Crystals", 2nd ed. (Robert E. Krieger, Malabar, Florida, 1977).
- (19) A. George and J. Rabier, *Revue. Phys. Appl.* 22, 1941 (1987)
- (20) R. Hull, J.C. Bean, L.J. Peticolas, D. Bahnck and B.E. Weir, to be published in *Proc. Mat. Res. Soc.* 263 (1992)
- (21) J.M. Bonar, R. Hull, R.J. Malik, R.W. Ryan and J.F. Walker, *Proc. Mat. Res. Soc.* 160, 117 (1990)
- (22) J.M. Bonar, R. Hull, J.F. Walker and R. Malik, *Appl. Phys. Lett.* 60, 1327 (1992)
- (23) R. Le Hazif and J.P. Poirier, *Acta. Metall.* 23, 865 (1975)
- (24) B. Pichaud, M. Burle and F. Minari, *Philos. Mag.* A44, 689 (1981)
- (25) C.-D. Qin and S.G. Roberts, in "Structure and Properties of Dislocations in Semiconductors 1989" (Institute of Physics, Bristol, England, 1989), p.321
- (26) M. Albrecht, H.P. Strunk, P.O. Hansson and E. Basuer, to be published in *Proc. Mat. Res. Soc.* 238 (1992)
- (27) M. Albrecht, H.P. Strunk, R. Hull and J.M. Bonar, to be published.